Enhancement of Ethanol Sensing Properties by Alloying TiO_2 With ZnO Tetrapods

Theerapong Santhaveesuk, Duangmanee Wongratanaphisan, and Supab Choopun

***Abstract*—The $Ti_xZn_{1-x}O$ tetrapods were synthesized using simple thermal oxidation method from Zn and TiO_2 mixture. The tetrapods exhibited single crystalline hexagonal wurtzite structure with the prefer growth direction of [0002] along the legs. The sensors based on $Ti_xZn_{1-x}O$ tetrapods were fabricated and investigated the ethanol sensing properties. The FE-SEM, HRTEM, SAED, XRD, and RS results suggested that $Ti_xZn_{1-x}O$ alloy was formed with a slightly decrease of c-axis lattice parameter. The decrease of sensor resistance under ethanol atmosphere was observed and suggested that the $Ti_xZn_{1-x}O$ tetrapods possessed n-type property of semiconductor similar to ZnO. The $Ti_xZn_{1-x}O$ tetrapod sensors exhibited higher sensitivity than that of pure ZnO tetrapod sensors for entire ethanol concentration with optimum operating temperature of 300 °C. Thus, the enhancement of sensitivity due to alloying TiO_2 with the ZnO tetrapods was observed and maybe explained by an increase of adsorbed oxygen ions due to substitution of Ti atom into Zn atom. Also, the slope value of the plot between $\log(S-1)$ and $\log C$ suggested that adsorbed oxygen ion species at the surface of the $Ti_xZn_{1-x}O$ tetrapods was O^{2-} which was same as pure ZnO tetrapods. Finally, these results have an important implication for a development of ethanol sensors based on metal oxide semiconductors for alcohol breath analyzer.**

***Index Terms*—Alloying, gas sensor, sensitivity, tetrapods.**

I. Introduction

ZNO metal oxide semiconductor with a direct wide-band gap (3.4 eV) and high excitation binding energy (60 meV) at room temperature [1] is well known as promising functional material. It has been widely used in many field areas, such as a light emitting diode [2], [3], transparent conducting oxide material [4], thermoelectric material [5], field emission device [6], and so on. Recently, alloy materials of ZnO with several elements have been investigated, such as Mg [7], Tb [2], Al [8], and Ce [9]. ZnO alloying with Ti and/or TiO_2 has also been received great interested due to wide range applications similar to ZnO. Chung *et al.* [10] have studied electrical and optical properties of TiO_2 doped ZnO films prepared by radio-frequency magnetron sputtering. It was found that TiO_2-doped ZnO film showed lower resistivity and higher band gap energy which can be used for transparent conducting oxide application. Also, Park and Ko [5] have studied thermoelectric property of $Ti_xZn_{1-x}O$ for thermoelectric generator application, and Xiong and Jiang [11] have investigated ferromagnetic property of Ti-doped ZnO for spintronic application. However, gas sensing property of $Ti_xZn_{1-x}O$ alloy for gas sensor application has been rarely reported especially ethanol sensor.

In this work, ethanol sensing properties of the $Ti_xZn_{1-x}O$ tetrapods prepared by simple thermal oxidation were investigated under ethanol concentration of 50–1000 ppm. The sensitivity of sensor was improved by the effect of TiO_2 alloying. The enhancement of the ethanol sensing properties was promising for application as alcohol breath analyzer.

II. Experimental

$Ti_xZn_{1-x}O$ tetrapods were synthesized by a simple thermal oxidation method. Zn and TiO_2 powders (Zn with 20 mol % of TiO_2) were weighed, mixed, and grounded in agate mortar for 2 h. Then, mixed powder in the amount of 2 g was loaded into an alumina crucible and put in the center of furnace at temperature of 1000 °C under normal atmosphere for a few minutes. The alumina crucible was taken out of the furnace, and the white wool products were observed. The synthesized products were characterized by field emission scanning electron microscope (FE-SEM), energy dispersive x-ray spectrometry (EDS), transmission electron microscope (TEM), X-ray diffractometer (XRD), and Raman spectrometry (RS) for morphology, chemical composition, phase formation, and crystal structure.

The tetrapods were fabricated as ethanol sensors by mixing tetrapods with polyvinyl alcohol, pasted onto the alumina substrate with gold inter-digital electrode to form thick films, and then dried in air for a few hours. The thick films were annealed at 400 °C under normal atmosphere for 4 h, and then cooled naturally to room temperature. The ethanol sensing response of the sensors was measured by using a volt-amperometric technique at the operating temperature of 240 °C–360 °C and at ethanol concentration of 50, 100, 200, 500, and 1000 ppm. Since application as alcohol breath analyzer was our goal, the ethanol vapor at various concentrations was generated from ethanol solution using alcohol simulator (GUTH laboratory Inc., Harrisburg USA). The alcohol simulator functioned to simulate alcohol concentration at conditions similar to exhaled human breath. The schematic diagram of ethanol sensing characteristic measurement was showed as in [12]. Typically, ethanol sensitivity (S) is defined as $R_{\rm air}/R_{\rm gas}$ [13], [14], where $R_{\rm air}$ is the electrical resistance of the sensor in air, and $R_{\rm gas}$ is its resistance in ethanol-air mixed gas.

Manuscript received November 15, 2008; revised January 28, 2009; accepted March 12, 2009. Current version published December 09, 2009. The work of T. Santhaveesuk was supported by Commission on Higher Education, Thailand, under the program Strategic Scholarships for Frontier Research Network for the Joint Ph.D. Program Thai Doctoral degree and Graduated School from Chiang Mai University. The work of S. Choopun was supported by Thailand Research Fund (TRF). The associate editor coordinating the review of this paper and recommending it for publication was Prof. Cristina Davis.

The authors are with the APRL, Department of Physics and Materials Science, Faculty of Science, Chiang Mai University, Chiang Mai 50200, Thailand and ThEP Center, CHE, Bangkok 10400, Thailand (e-mail: supab@science.cmu.ac.th; s_theerapong@yahoo.co.th; dwongrat@chiangmai.ac.th).

Color versions of one or more of the figures in this paper are available online at http://ieeexplore.ieee.org.

Digital Object Identifier 10.1109/JSEN.2009.2036048

1530-437X/$26.00 © 2009 IEEE

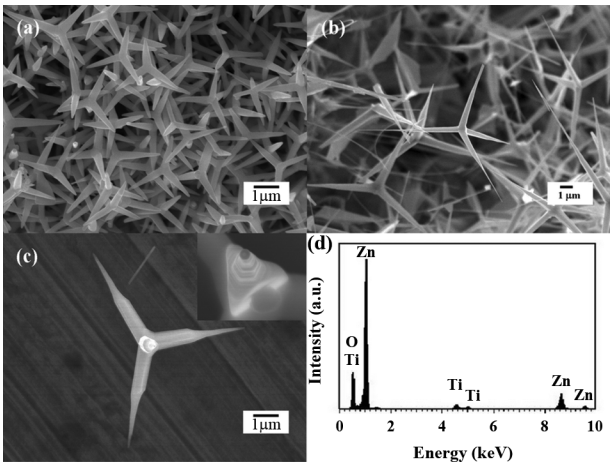

Fig. 1. FE-SEM images of the $\mathrm{Ti}_x\mathrm{Zn}_{1-x}\mathrm{O}$ tetrapods with (a) the round tip type, (b) the sharp tip type, and (c) high magnified FE-SEM image of one tetrapod with hexagonal tip shown in inset (d) EDS spectrum of $\mathrm{Ti}_x\mathrm{Zn}_{1-x}\mathrm{O}$ tetrapods.

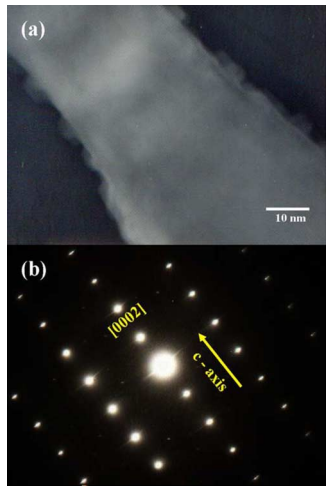

Fig. 2. (a) HRTEM image of the selected leg of the $\mathrm{Ti}_x\mathrm{Zn}_{1-x}\mathrm{O}$ tetrapod and (b) The corresponding SAED pattern.

TABLE I
LIST OF CHEMICAL COMPOSITION OF THREE TETRAPODS

Sample	Chemical composition (at.%)		
	Zn	O	Ti
Tetrapod 1 (sharp tip)	49.9	50.0	0.1
Tetrapod 2 (round tip)	47.0	52.7	0.3
Tetrapod 3 (round tip)	49.4	49.7	0.9
Average	48.7±1.5	50.8±1.6	0.4±0.4

III. RESULTS AND DISCUSSIONS

A. *Characterization of* $\mathrm{Ti}_X\mathrm{Zn}_{1-x}\mathrm{O}$ *Tetrapods*

FE-SEM micrographs of the tetrapods synthesized from Zn and TiO_2 mixture using simple thermal oxidation method are shown in Fig. 1. As illustrated in Fig. 1(a), the tetrapods are observed with four symmetric legs. It is clearly seen that there are two different types of tetrapods; round tip type and sharp tip type as shown in Fig. 1(a) and 1(b), respectively. The round tip tetrapods have the length of 1–2 μm and the diameter of 160–280 nm whereas the sharp tip tetrapods have the length of 3–13 μm and the diameter of 330–470 nm. The high magnified FE-SEM image of one tetrapod as shown in Fig. 1(c) exhibits needle-like shape with a hexagonal tip (see inset). EDS spectrum of the tetrapod is shown in Fig. 1(d) with the spot size in an order of micrometer. The spectrum shows Zn, Ti, and O signals indicating the tetrapod consists of Zn, Ti and O elements. This suggests that Ti is in tetrapod and incorporated into ZnO. The atomic percent of each element is revealed in Table I for three tetrapods. The average atomic percent of each element is found to be 0.4 ± 0.4, 48.7 ± 1.5, and 50.8 ± 1.6 for Ti, Zn, and O, respectively. It should be noted that this EDS analysis was qualitative analysis. For quantitative analysis, it will need other technique such as inductive coupled plasma mass spectroscopy (ICP-MS).

Fig. 2(a) shows a representative HRTEM image of the selected leg of the tetrapod. Fig. 2(b) shows SAED (selected area electron diffraction) pattern associated to HRTEM in Fig. 2(a). A spot pattern is obtained indicating the $\mathrm{Ti}_x\mathrm{Zn}_{1-x}\mathrm{O}$ tetrapods are a single crystal with high degree of crystalinity corresponding to wurtzite structure of ZnO. Moreover, only spots corresponding to ZnO structure are observed implying no structure changes due to mixing ZnO with TiO_2 and Ti atom should substitute into Zn atom site to form $\mathrm{Ti}_x\mathrm{Zn}_{1-x}\mathrm{O}$ alloy. Ti^{4+} trends to substitute into Zn^{2+} sites since Ti^{4+} has ionic radius of 0.068 nm which smaller than that 0.074 nm of Zn^{2+} [5], [14]. From the trace analysis, it is found that the $\mathrm{Ti}_x\mathrm{Zn}_{1-x}\mathrm{O}$ tetrapods grow along $[0002]$ direction which is a typical growth direction for hexagonal ZnO [3], [15], [16].

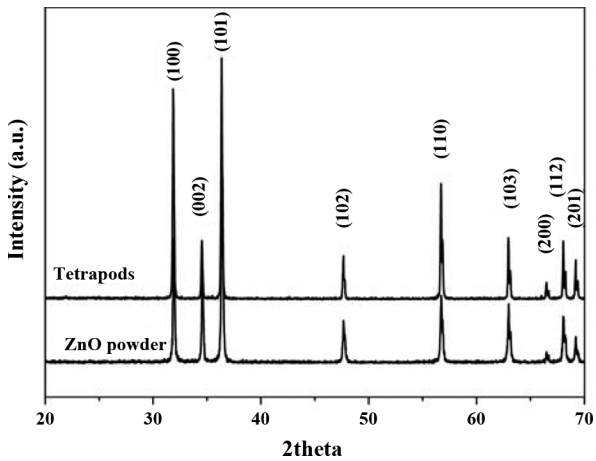

Fig. 3. XRD pattern of the $\mathrm{Ti}_x\mathrm{Zn}_{1-x}\mathrm{O}$ tetrapods compared with that of ZnO powder.

The typical XRD pattern of the $\mathrm{Ti}_x\mathrm{Zn}_{1-x}\mathrm{O}$ tetrapods scanning for a value of 20°–70° is illustrated in Fig. 3, compared with ZnO powder. The pattern shows well crystallized diffraction peaks identical to ZnO powder. No other impurity peak is observed in the pattern. Such the strong and sharp peaks in the pattern corresponding to planes (100), (002), (101), (102), (110), (103), (200), (112), and (201), respectively, the peaks can be indexed to a hexagonal wurtzite ZnO structure [17].

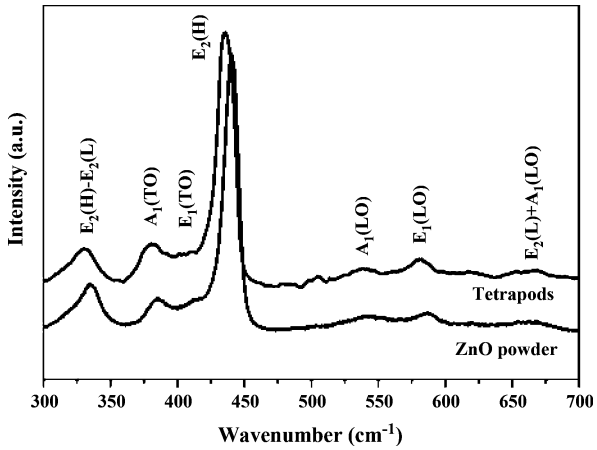

Fig. 4. Raman spectrum of the $Ti_xZn_{1-x}O$ tetrapods compared with that of ZnO powder.

This result is in good agreement with the FE-SEM, HRTEM, SAED, and EDS results. The lattice parameter a of $Ti_xZn_{1-x}O$ tetrapods is 3.248 Å whereas c is 5.192 Å, respectively. The value of lattice parameter c of the tetrapods is slightly smaller than that of data in standard file [17]. This result indicates that Ti atom substituted into ZnO lattice to form $Ti_xZn_{1-x}O$ alloy consenting with the EDS result.

Raman spectrum of the $Ti_xZn_{1-x}O$ tetrapod at room temperature is displayed in Fig. 4 with Raman spectrum of ZnO powder for comparison. It is clearly seen that all peaks of Raman shift of the $Ti_xZn_{1-x}O$ tetrapods is well agreement with ZnO powder and can be attributed to hexagonal ZnO structures. The vibration mode of 331 cm^{-1} can be assigned to the second order Raman spectrum arising from zone-boundary phonons $E_2(H) - E_2(L)$ mode [18], whereas the strongest and sharpest peak centered at 435 cm^{-1} can be assigned to $E_2(H)$ mode. This mode is the intrinsic characteristic of wurtzite hexagonal ZnO [16], [18], [19]. The peak located at 582 cm^{-1} is ascribed to $E_1(LO)$ mode of the ZnO. The peak at 381 cm^{-1} corresponds to $A_1(TO)$ and at 411 cm^{-1} corresponds to $E_1(TO)$, respectively [2], [16]. In addition, $A_1(LO)$ mode [16] can be observed in the spectrum, position at 539 cm^{-1} whereas the Raman peak center at 666 cm^{-1} can be assigned to $E_2(L) + A_1(LO)$ mode [20].

Moreover, compared to ZnO powder, all Raman peaks of the tetrapods shift to lower wavenumber, and the $E_2(H)$ peak is broader. These imply that Ti^{4+} replaced into Zn^{2+} sites in ZnO lattice [2], [4], [10]. The Ti substitution result is well consistence with those XRD, HRTEM, SAED, and EDS data and it is in agreement with other reports [5], [10].

B. Ethanol Sensing Properties

The plot of resistance of sensor versus time is illustrated in Fig. 5(a) under the ethanol concentration of 1000 ppm at various operating temperature. The resistance of sensor is high in air, but drops sharply when exposed to the ethanol atmosphere. The decrease of resistance under ethanol atmosphere suggests that the $Ti_xZn_{1-x}O$ tetrapods possess n-type property of semiconductor similar to ZnO. The sensor is left in ethanol-air mixed gas

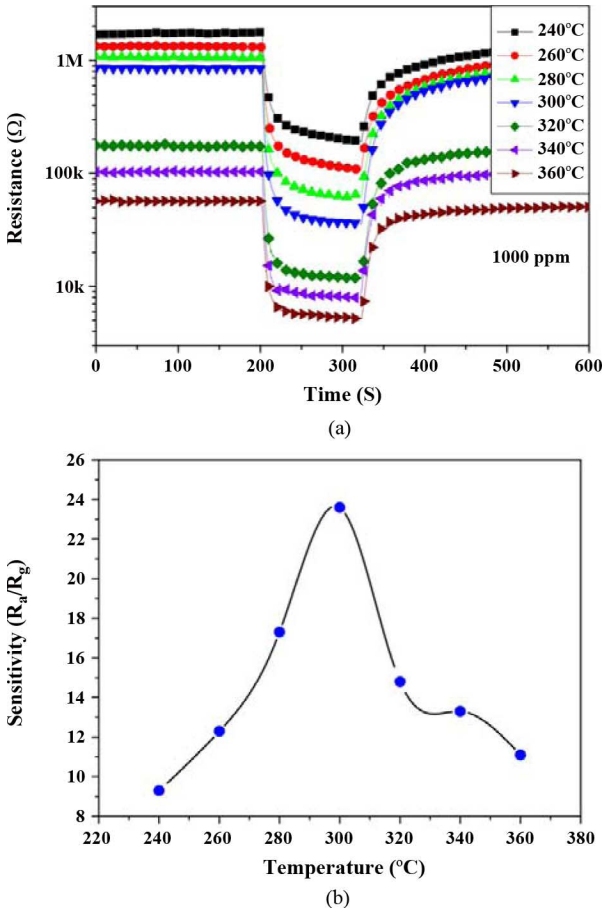

Fig. 5. (a) Plot of resistance of sensor versus time under the ethanol concentration of 1000 ppm at various operating temperature and (b) Plot of sensor sensitivity as a function of operating temperature at ethanol concentration of 1000 ppm.

for 120 s, and then switches to air again. As a result, the resistance of sensor increases as the decreased of the ethanol concentration in testing chamber. For example, at 280 °C the resistance of sensor reduces from 1 MΩ (in air) to about 63 kΩ (in ethanol ambient). The similar response behavior is observed for most metal oxide semiconductor sensors [13], [14], [21], [22]. It is well-known that gas sensing mechanism of the most metal oxide semiconductor sensors is based on adsorption between oxygen ions on the surface of sensor and target gas [14], [21]. Thus, it is likely that the same mechanism occurs for our tetrapod sensor. When the sensor expose to air, oxygen molecules adsorb on the surface of tetrapods to form oxygen ions and act as electron acceptor leading to high resistivity. The trapped electrons are released back to the surface of sensor as the ethanol molecules react with oxygen ions on the surface resulting in low resistivity.

The returning to the initial value of the sensor resistance is observed in all samples, depended on the concentration and operating temperature. At low concentration (50, 100 ppm), it is in an order of a few tens second to a hundred second. At high ethanol concentration (above 100 ppm), it is in an order of 500 s. For example, the sensor exposed to 50 ppm and 100 ppm of ethanol concentration at 280 °C took about 169 s and 188 s to return to the initial value, whereas sensor tested at 300 °C took about 70 s and 90 s for ethanol concentration of 50 ppm and 100 ppm, respectively. For higher ethanol concentration (1000 ppm), the

TABLE II
SENSITIVITIES OF $Ti_xZn_{1-x}O$ TETRAPOD SENSORS AT 280 °C, 300 °C, AND 320°C COMPARED WITH THAT OF PURE ZNO TETRAPOD SENSOR AT 300 °C

Ethanol concentration	Sensitivity			
	280°C	300°C	300°C in [22]	320°C
50 ppm	5.3	5.0	1.2	5.4
100 ppm	6.7	6.3	1.4	6.4
200 ppm	8.5	8.9	1.5	8.0
500 ppm	12.7	16.4	1.7	11.9
1000 ppm	17.3	23.6	1.8	14.8

sensor returned to the initial state, however it will take longer time than that of the data showing in Fig. 5(a). It took about 500 s for test at 300°C.

Fig. 5(b) shows plot of sensor sensitivity as a function of operating temperature at ethanol concentration of 1000 ppm. The sensor sensitivity increase as increasing the operating temperature, and reaches the optimized value of about 23.6 at 300 °C. At the operating temperature higher than 300 °C, the sensor sensitivity decreases to 11.1 at 360 °C. At different ethanol concentration, the sensor sensitivities at 280 °C, 300 °C, and 320 °C are listed in Table II. It can be clearly seen that the sensitivities have maximum value at approximately 300 °C for entire ethanol concentration indicating an optimum operating temperature of 300 °C.

For comparison, the sensitivities of sensor based on pure ZnO tetrapods are also put in Table II. It can be clearly seen that the $Ti_xZn_{1-x}O$ tetrapod sensors exhibit higher sensitivity than that of pure ZnO tetrapod sensors for entire ethanol concentration. For example, the sensitivity of the $Ti_xZn_{1-x}O$ tetrapod sensor is about 13 times higher than that of the pure ZnO tetrapod sensor [22] at 1000 ppm. Thus, the enhancement of sensitivity due to alloying TiO_2 with the ZnO tetrapods is clearly observed. This sensitivity enhancement may be explained by a substitution of Ti atom into Zn atom. When Ti atom substituted into Zn sites in ZnO lattice, two electrons of Ti atom bond with oxygen atom, and other two electrons become relatively free electrons. These titanium ions with two free electrons can react with more oxygen molecule in air and results in higher oxygen ions on the $Ti_xZn_{1-x}O$ tetrapod surface. Therefore, the higher adsorbed oxygen ions can react with larger number of ethanol molecule and results in higher sensitivity. The sensor recovery time of the $Ti_xZn_{1-x}O$ tetrapod sensor increased with the increased of ethanol concentration. Compared to pure ZnO tetrapods, our sensor recovery times are longer.

Additionally, the sensitivity of the metal oxide semiconductor normally can be written as $S = 1 + aC^b$ [23], [24], where C is a gas concentration, a is a constant depending on type of test gas, sensor material, and operating temperature whereas b is generally equal to 0.5 or 1 for adsorbed surface oxygen species of O^{2-} or O^-, respectively. Thus, by plotting between $\log(S-1)$ and $\log C$, the value of b can be achieved on a slope of this plot. The plot between $\log(S-1)$ and $\log C$ for $Ti_xZn_{1-x}O$ sensors operated at 300 °C is showed in Fig. 6. The linear relation can be observed with a slope of 0.59 and thus, b value is 0.59 which is close to 0.5. This implies that the adsorbed oxygen species on the surface of $Ti_xZn_{1-x}O$ sensors is O^{2-} which is the same as pure ZnO [25]. It should be noted that the adsorbed surface oxygen species does not change by alloying TiO_2 with ZnO.

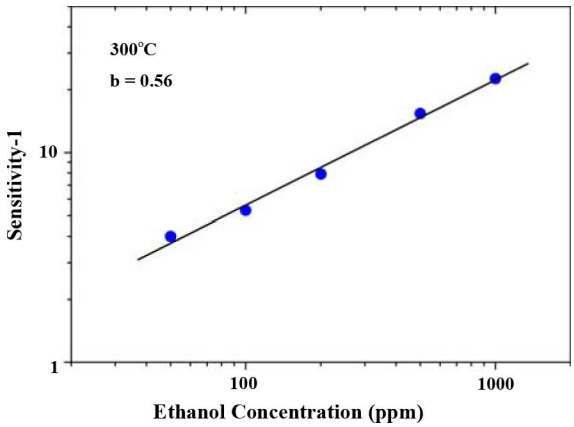

Fig. 6. Plot between $\log(S-1)$ and $\log C$ for $Ti_xZn_{1-x}O$ tetrapod sensors operated at 300 °C.

IV. CONCLUSION

The sensors based on $Ti_xZn_{1-x}O$ tetrapods were fabricated and investigated the ethanol sensing properties. The FE-SEM, HRTEM, SAED, XRD, and RS results, suggested that $Ti_xZn_{1-x}O$ alloy was formed with a slightly decrease of c-axis lattice parameter. The decrease of sensor resistance under ethanol atmosphere was observed and suggested that the $Ti_xZn_{1-x}O$ tetrapods possessed n-type property of semiconductor similar to ZnO. The enhancement of sensitivity due to alloying TiO_2 with the ZnO tetrapod was observed and maybe explained by an increase of adsorbed oxygen ions due to substitution of Ti atom into Zn atom. Also, the slope value of the plot between $\log(S-1)$ and $\log C$ suggested that adsorbed oxygen ion species at the surface of the $Ti_xZn_{1-x}O$ tetrapods was O^{2-} which was same as pure ZnO tetrapod. Finally, these results have an important implication for a development of ethanol sensors based on metal oxide semiconductors for alcohol breath analyzer.

ACKNOWLEDGMENT

The authors would like to thank Electro Ceramics (Thailand) Co., Ltd. for supporting alumina substrate.

REFERENCES

[1] V. A. Coleman and C. Jagadish, "Basic properies and applications of ZnO," in *Zinc Oxide Bulk, Thin Films and Nanostructure: Processing, Properties and Application*, C. Jagadish and S. Pearton, Eds. Oxford, U.K.: Elsevier Science, 2006, ch. 1, pp. 1–20.

[2] L. Yang, Y. Tang, A. Hu, X. Chen, K. Liang, and L. Zhang, "Raman scattering and luminescence study on arrays of ZnO doped with Tb^{3+}," *Physica B*, vol. 403, pp. 2230–2234, 2008.

[3] F. Wang, Z. Ye, D. Ma, L. Zhu, and F. Zhuge, "Rapid synthesis and photoluminescence of novel ZnO nanotetrapods," *J. Cryst. Growth*, vol. 274, pp. 447–452, 2005.

[4] J. J. Lu, Y. M. Lu, S. I. Tasi, T. L. Hsiung, H. P. Wang, and L. Y. Jang, "Conductivity enhancement and semiconductor-metal transition in Ti-doped ZnO films," *Opt. Mater.*, vol. 29, pp. 1548–1552, 2007.

[5] K. Park and K. Y. Ko, "Effect of TiO_2 on high-temperature thermoelectric properties of ZnO," *J. Alloy. Compd.*, vol. 430, pp. 200–204, 2007.

[6] K. Zheng, H. Shen, J. Li, D. Sun, G. Chen, K. Hou, C. Li, and W. Lei, "The fabrication and properties of field emission display based on ZnO tetrapod-liked nanostructure," *Vacuum*, vol. 83, pp. 261–264, 2009.
[7] S. Choopun, R. D. Vispute, W. Yang, R. P. Sharma, T. Venkatesan, and H. Shen, "Realization of band gap above 5.0 eV in metastable cubic-phase $Mg_xZn_{1-x}O$ alloy films," *Appl. Phys. Lett.*, vol. 80, pp. 1529–1531, 2002.
[8] X. Y. Zue, L. M. Li, H. C. Yu, Y. J. Chen, Y. G. Wang, and T. H. Wang, "Extremely stable field emission from AlZnO nanowire arrays," *Appl. Phys. Lett*, vol. 89, pp. 043113–043118, 2006.
[9] B. Cheng, Y. Xiao, G. Wu, and L. Zhang, "The vibrational properties of one-dimensional ZnO:Ce nanostructures," *Appl. Phys. Lett*, vol. 84, pp. 416–418, 2004.
[10] J. L. Chung, J. C. Chen, and C. J. Tseng, "Electrical and optical properties of TiO_2-doped ZnO films prepared by radio-frequency magnetron sputtering," *J. Phys. Chem. Solids*, vol. 69, pp. 535–539, 2008.
[11] Z. H. Xiong and F. Y. Jiang, "First-principles study of electronic structure and ferromagnetism in Ti-doped ZnO," *J. Phys. Chem. Solids*, vol. 68, pp. 1500–1503, 2007.
[12] N. Hongsith and S. Choopun, *Enhancement of Ethanol Sensing Properties by Impregnating Platinum on Surface of ZnO Tetrapods*, unpublished.
[13] T. Santhaveesuk, D. Wongratanaphisan, and S. Choopun, *Growth and Ethanol Response of* $Zn-TiO_2$ *Nanostructures Using Thermal Oxidation Method*, unpublished.
[14] Q. Wan, Q. H. Li, Y. J. Chen, T. H. Wang, X. L. He, J. P. Li, and C. L. Lin, "Fabrication and ethanol sensing characteristics of ZnO nanowire gas sensors," *Appl. Phys. Lett.*, vol. 84, pp. 3654–3656, 2004.
[15] C. C. Li, Z. F. Du, L. M. Li, H. C. Yu, Q. Wan, and T. H. Wang, "Surface-depletion controlled gas sensing of ZnO nanorods grown at room temperature," *Appl. Phys. Lett.*, vol. 91, pp. 032101–032103, 2007.
[16] S. H. Huang, Z. Chen, X. C. Shen, Z. Q. Zhu, and K. Yu, "Raman scattering of single tetrapod-like ZnO nanostructure synthesized by catalyst-free rapid evaporation," *Solid State Commun.*, vol. 145, pp. 418–422, 2008.
[17] *Joint Committee on Powder Diffraction Standards (JCPDS)*, , 36-1451.
[18] S. J. Chen, Y. C. Liu, Y. M. Lu, J. Y. Zhang, D. Z. Shen, and X. W. Fan, "Photoluminescence and Raman behaviors of ZnO nanostructures with different morphologies," *J. Cryst. Growth*, vol. 289, pp. 55–58, 2006.
[19] Y. Huang, M. Liu, Z. Li, Y. Zeng, and S. Liu, "Raman spectroscopy study of ZnO-based ceramic films fabricated by novel sol-gel process," *Mat. Sci. Eng. B*, vol. 97, pp. 111–116, 2003.
[20] D. Shuang, J. B. Wang, X. L. Zhong, and H. L. Yan, "Raman scattering and cathodoluminescence properties of flower-like manganese doped ZnO nanorods," *Mater. Sci. Semicond. Process.*, vol. 10, pp. 97–102, 2007.
[21] X. Y. Xue, Y. J. Chen, Y. G. Liu, S. L. Shi, Y. G. Wang, and T. H. Wang, "Synthesis and ethanol sensing properties of indium-doped tin oxide nanowires," *Appl. Phys. Lett.*, vol. 88, p. 201907, 2006.
[22] N. Hongsith and S. Choopun, "Effect of platinum impregnation on ZnO tetrapods for ethanol sensor," *Adv. Mater. Res.*, vol. 55–57, pp. 289–292, 2008.
[23] D. E. Williams, "Semiconducting oxides as gas-sensitive resistors," *Sens. Actuators B*, vol. 57, pp. 1–16, 1999.
[24] N. Hongsith, E. Wongrat, T. Kerdcharoen, and S. Choopun, "Sensor response formula for sensor based on ZnO nanostructures," *Sens. Actuators B*.
[25] S. Choopun, N. Hongsith, P. Mangkorntong, and N. Mangkorntong, "Zinc oxide nanobelts by RF sputtering for ethanol sensor," *Physica E*, vol. 39, pp. 53–56, 2007.

Theerapong Santhaveesuk received the B.Ed. degree in physics in 1999 and the M.Sc. degree in physics from Chiang Mai University, Chiang Mai, Thailand, in 2002. He is currently working towards the Ph.D. degree in materials science at Chiang Mai University.

His current research interests include growth and characterization of $Zn-TiO_2$ compound in nanostructure for gas sensor applications.

Duangmanee Wongratanaphisan received the Ph.D. degree in physics from Lehigh University, Lehigh, PA, in 2003.

She has worked on ferroelectric crystals $(Pb(Zn_{1/3}Nb_{2/3})O_3 - PbTiO_3)$ and metal oxide semiconductors $(Zn-TiO_2)$. She is currently an Assistant Professor with the Department Physics and Materials Science, Faculty of Science, Chiang Mai University, Thailand.

Supab Choopun received the Ph.D. degree in chemical physics from the University of Maryland, College Park, in 2002.

Currently, he is an Assistant Professor with the Department of Physics and Materials Science, Faculty of Science, Chiang Mai University, Thailand. His current research interests are in the field of metal oxide semiconductor nanostructures such as ZnO for gas sensor and dye-sensitized solar cell applications.